Plasma Immersion Ion Implantation with Solid Targets for Space and Aerospace Applications

R. M. Oliveira[1], J. A. N. Gonçalves[1], M. Ueda[1], G. Silva[1], K. Baba[2]

[1] *National Institute for Space Research, PO Box 515, ZIP 12227-010*
São José dos Campos, São Paulo, Brazil, email: rogerio@plasma.inpe.br

[2] *Industrial Technology Center of Nagasaki, 2-1303-8, Ikeda, Omura*
Nagasaki 856-0026, Japan

Abstract

This paper describes successful results obtained by a new type of plasma source, named as Vaporization of Solid Targets (VAST), for treatment of materials for space and aerospace applications, by means of plasma immersion ion implantation and deposition (PIII&D). Here, the solid element is vaporized in a high pressure glow discharge, being further ionized and implanted/deposited in a low pressure cycle, with the aid of an extra electrode. First experiments in VAST were run using lithium as the solid target. Samples of silicon and aluminum alloy (2024) were immersed into highly ionized lithium plasma, whose density was measured by a double Langmuir probe. Measurements performed with scanning electron microscopy (SEM) showed clear modification of the cross-sectioned treated silicon samples. X-ray photoelectron spectroscopy (XPS) analysis revealed that lithium was implanted/deposited into/onto the surface of the silicon. Implantation depth profiles may vary according to the condition of operation of VAST. One direct application of this treatment concerns the protection against radiation damage for silicon solar cells. For the case of the aluminum alloy, X-ray diffraction analysis indicated the appearance of prominent new peaks. Surface modification of Al2024 by lithium implantation/deposition can lower the coefficient of friction and improve the resistance to fatigue of this alloy. Recently, cadmium was vaporized and ionized in VAST. The main benefit of this element is associated with the improvement of corrosion resistance of metallic substrates. Besides lithium and cadmium, VAST allows to performing PIII&D with other species, leading to the modification of the near-surface of materials for distinct purposes, including applications in the space and aerospace areas.

CP 1087, *Protection of Materials and Structures from Space Environment, Proceedings of the 9th International Conference: Protection of Materials and Structures from Space Environment*, edited by J. I. Kleiman

1. Introduction

Most of the materials used in space and aerospace applications, regardless of being polymeric, metallic or semiconductor, require some kind of treatment to face the harsh space environment they are submitted.

Plasma immersion ion implantation and deposition (PIII&D) is an effective method to treat the surface of a variety of materials [1-3], including those for space and aerospace areas. A significant advantage of this process in comparison with beamline ion implantation[4] is its non line-of-sight characteristic that allows the treatment of complex surfaces without target manipulation. Nevertheless, this approach is sometimes limited by the type of the plasma source used, usually produced by means of gaseous discharges of nitrogen or carbon. In order to meet the demands for new material requirements, it is essential to consider new plasma sources, especially those ones using solid elements, as needed for treatments with many metallic species. This is an important issue because metal-ion implantation has shown significant advantages over gaseous ion implantation in several applications [5]. In particular, the implantation and/or deposition of metallic species into/onto the surface of materials used for space and aerospace applications can significantly improve their characteristics.

This paper reports about a process of PIII&D performed on samples of silicon and aluminum alloy (2024), using lithium ions. The lithium plasma was produced in a Vaporization of Solid Targets (VAST) source after the vaporization of solid lithium [6].

Implantation of lithium in silicon is intended to improve the resistance to radiation damage of a silicon solar cell. The purpose is to treat the cell's base region, where most of radiation damage occurs. Even though lithium is an n-dopant in silicon, the main purpose is to introduce lithium in controlled quantities so that the cell base remains p-type. It is well known that p-type silicon is innately more radiation damage resistant than n-type silicon. In the case of aluminum, the implantation/deposition of lithium can change its surface properties, lowering the coefficient of friction and improving the resistance to fatigue of this alloy.

2. Experimental

The process of PIII&D using VAST makes use of a glow discharge running in high and low pressure values, in which argon played the role of the carrier of the gas and the heater of a crucible containing the solid element (lithium). The experimental apparatus is shown in figure 1[7].

To start the process, initially argon gas fills 60 liters by volume vacuum chamber until a pressure of approximately 1 mbar is established. An argon glow discharge is turned on when the cathode, consisting of a conic molybdenum crucible 2 cm deep and hosting small pieces of metallic lithium, is negatively polarized by a DC voltage ranging from 400V to 1kV. For this condition, the plasma remains concentrated around the electrode. The high flux of argon ions reaching the cathode leads to a fast heating of the target. The temperature of the crucible reaches 400 °C easily, which is much higher than the melting point of the lithium (180 °C).

Once evaporated, lithium atoms are ionized due to collisions with plasma particles. The process is self-sustained and, as the lithium is being evaporated and ionized, more ion collisions happen, causing further increase of the temperature of the crucible and higher evaporation rate of lithium, as previously predicted [8,9]. If the pressure of the discharge and the polarization of the electrode remain constant, the temperature of the crucible begins to increase exponentially. In fact, temperatures as high as 800 °C were measured by an optical pyrometer viewing the crucible through a side glass window. Even though very high lithium evaporation rate occurs for this case, the pressure of the discharge is reduced to 6 x 10^{-3} mbar in order to allow the plasma to spread out to fill the processing chamber steadily.

The pumping system which is composed of a two-stage rotary pump (10 m^3/h), a mechanical booster pump based on Roots principle (375 m^3/h) and a diffusion pump allows for the operation pressure to remain in the range of 6 x 10^{-3} mbar to 1 mbar, for the whole process.

When the operation pressure is decreased to 6 x 10^{-3} mbar, the other electrode (anode) is positively polarized to further ionize the metal vapor. For this case, negative

voltage pulses (6kV/6μs/3kHz), supplied by a Compact High Voltage Pulser (CHVP) [10,11], are applied to the Si samples, causing lithium base coating and implantation. CHVP can supply pulses of up to 20 kV but with reduced duty cycle. The degree of ionization changed significantly after lithium vaporization, since plasma density measured by double Langmuir probe varied from a maximum of 4×10^{-9} mbar to 1×10^{10} mbar.

Silicon test samples were investigated using high resolution x-ray diffraction analysis. The X-ray diffraction measurements were carried out in a Phillips X'Pert diffractometer equipped with a four-crystal Ge(220) monochromator in the primary optics (between the Cu X-ray tube and the sample). In this configuration, the incident X-ray beam has an axial divergence of 12 arcsec and a wavelength dispersion of approximately 2×10^{-4}. An open detector in the secondary optics detected the diffracted beam. W-Scans around the Si(004) diffraction peak with the detector fixed at the 2Θ Bragg angle (rocking curve) were performed on the Si wafers before and after lithium implantation.

X-ray photoelectron spectrometry was performed in a Shimadzu ESCA-1000 device. Surface analysis was carried out using a JSM 5310 Scanning Electron Microscope.

3. Results and Discussion

The effect of ion implantation in silicon substrate can be verified by means of high resolution X-ray diffraction measurements [12]. In fact, such measurements are strongly affected by the strain distribution created both by ions and damage in the implanted region [13,14]. The rocking curve for a silicon sample immersed into the lithium plasma produced in VAST during 50 minutes, under an operation pressure of 6×10^{-3} mbar and polarized by pulses of 6.5 kV/2.5 kHz/7μs, indicated a clear distortion in comparison to the symmetrical curve for the untreated sample, as can be seen in figure 2.This first evidence of ion implantation was further confirmed by SEM and XPS measurements.

Scanning electron microscopy (SEM) analysis using a backscattering electrons' detector was used to view the cross-section of a silicon sample implanted with lithium atoms using VAST. THE SEM analysis revealed the formation of a uniform layer of 0.19 μm in thickness below a coated surface of approximately 0.23 μm, as can be seen in figure 3. In

the SEM images in figure 3, the clearer regions are identified as the ones with higher conductivity. Therefore, the presence of lithium, a metallic element, is distinguished from the silicon, a semiconductor, by the contrast of the image. The thickness of both regions may vary, according to the conditions of treatment of VAST. By varying the pressure of the discharge and the temperature of the crucible, the thickness of the clearer regions, results not shown here, may vary significantly, reaching values from tens of nanometers up to 2 μm.

The atomic concentration of lithium implanted into silicon sample reached a maximum of 75% as measured by XPS at the free surface. A gradual decrease of lithium concentration with time of etching was observed, with the Li concentration reaching practically zero after about 70 minutes of etching, as can be seen in figure 4a. Inversely, the concentration of silicon increases with the increase of the etching time, denoting the process of lithium implantation. Oxygen is a contaminant in this case and its presence is also due to the process of lithium oxidation. The etching rate that was used during XPS depth profile measurements was 3.3 nm/min and was calibrated by SiO_2.

Figure 4b and 4c show distinct intensities of the binding energy for Li 1s (54.7 eV)[15,16] and Si 2p (99.2 eV)[17], respectively, versus the etching time. For lithium case, first curves mainly concern Li_2O ionic binding, changing to Li – Li and to Li-Si, metallic bindings. As it was expected, the intensities decreased and vanished with the penetration depth, due to the absence of lithium element for inner layers. It is worthwhile to verify a slight shift of the peak of the binding energy for lithium from higher values to smaller ones, due to the kind of binding of lithium with oxygen first, lithium and silicon afterwards, according to the evolution of the etching time. For Si case, the intensity of the first lines is negligible, due to the high concentration of lithium and the presence of oxygen in the near surface. The decrease of the intensity of these elements explains the increase of the intensity of silicon lines for greater etching times. Here, a shift of the binding energy to lower values occurs. This is probably due to the presence of silicon oxide in outer regions, in comparison to the binding energy of silicon-silicon for the inner layer.

Lithium was also implanted in aluminum alloy Al2024. First measurements were made in such samples in order to verify the presence of lithium atoms by means of X-ray diffraction. Prominent new peaks, distinct from the ones present in untreated sample of

Al2024, appeared in the x-ray diffraction patterns, as shown in figure 5. This figure shows the diffracted lines for pure lithium, pure aluminum alloy and for three samples of the alloy submitted to PIII&D with lithium atoms in VAST. It can be observed that all the peaks of pure aluminum are present in the treated samples. Otherwise, the main peaks for lithium (36° and 52°) were suppressed in the treated samples.

This is due to the fact that lithium diffuses in the crystal cell of the aluminum and, therefore, there are no peaks of its main crystallographic plane. The bands shown in this diffractogram may be due to oxides of different coordinate numbers and hydration, since lithium fast reacts with oxygen and moisture in the air.

New planes, absent from the pure aluminum and lithium, are present in diffractograms of the implanted samples. This may be explained due to the low atomic weight of lithium that occupies interstitial spaces, originating crystalline planes not present in the pure elements. Additionally, it can be verified that the main aluminum planes are intensified, showing that lithium also occupies interstitial spaces in aluminum in the same preferential planes.

4. Summary

VAST is a new plasma source that was designed to perform PIII&D by means of the vaporization of solid targets. In the experiment reported in this paper, lithium was vaporized and ionized in VAST and implanted in silicon and aluminum substrates. For silicon samples, high resolution X-ray diffraction analysis revealed clear asymmetry of the curve obtained for the treated sample in comparison with the untreated one, as a result of the lithium implantation. SEM measurements showed a distinct outer layer hundreds of nanometers thick due to the presence of lithium, in contrast with the pure silicon substrate. In addition, XPS results indicated atomic concentration of lithium of 75% in the near surface and a gradual decrease afterwards. For aluminum alloy, X-ray diffraction showed the presence of prominent new peaks due to the treatment with lithium atoms. In brief, VAST was able to perform PIII&D in silicon and aluminum alloy with lithium atoms, a kind of treatment of interest for space and aerospace areas. By modifying the conditions of treatment, mainly concerning to the characteristics of the pulse applied to the samples, it is possible to create different implantation profiles. This would be the next necessary

experimental step, to find the best conditions in VAST to treat the base of silicon solar cells and specimen of aluminum alloy 2024.

5. Acknowledgments

This work was supported by Fapesp

FIGURES

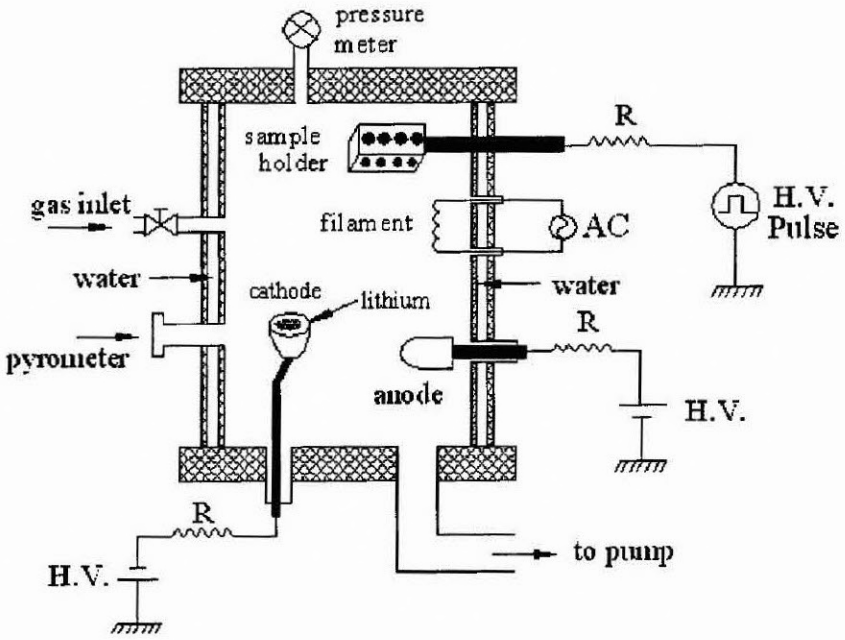

Figure 1. Schematic drawing of VAST

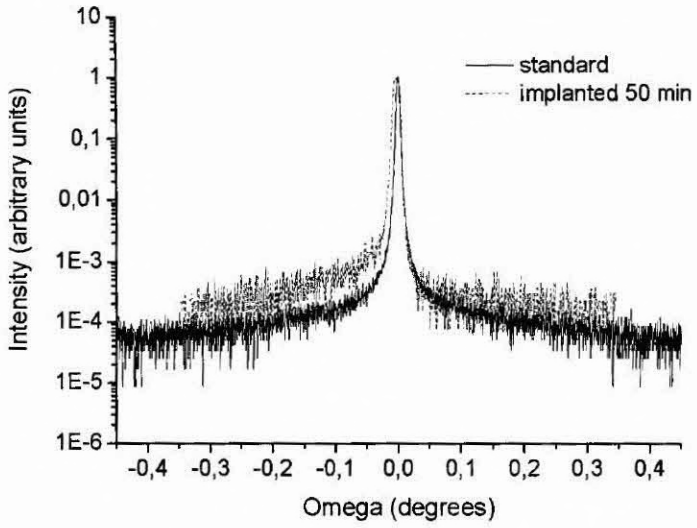

Figure 2. Rocking curve for silicon sample treated by PIII&D with lithium ions in comparison with untreated Si substrate.

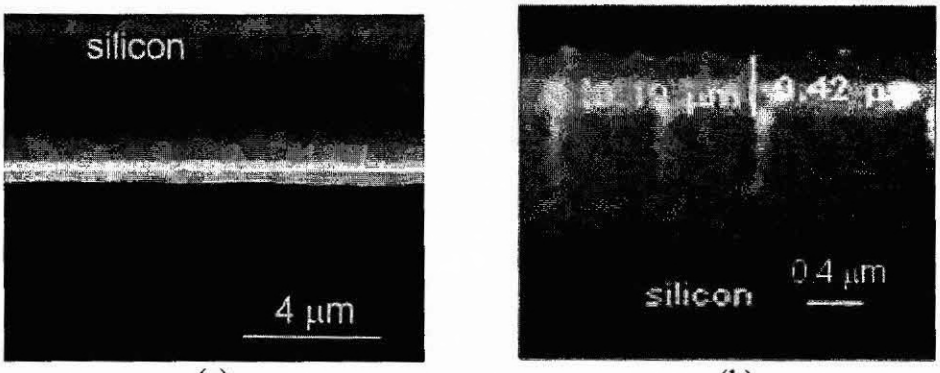

(a) (b)

Figure 3. SEM image of the cross section of a silicon sample implanted with lithium atoms. (a) magnification of 10,000 ; (b) magnification of 50,000

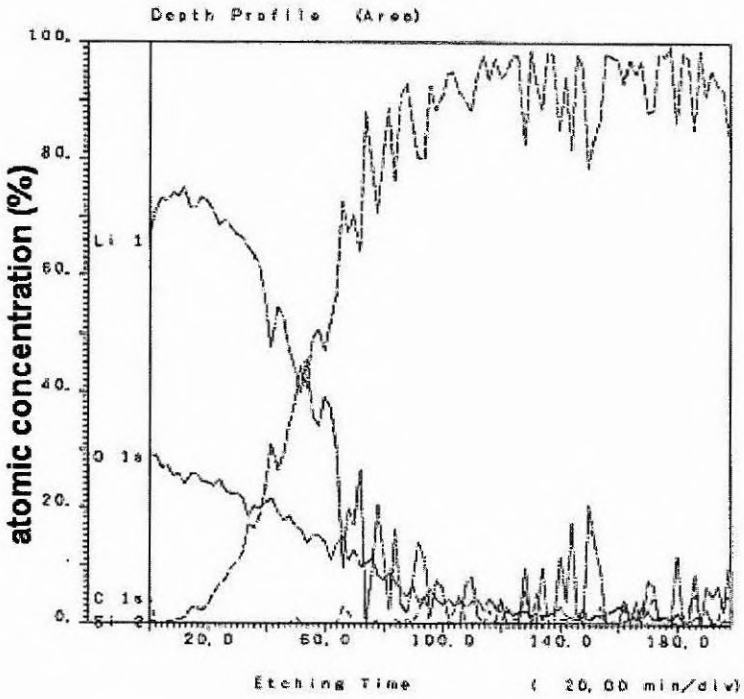
Depth Profile (Area)
atomic concentration (%)
100.
80.
60.
40.
20.
0.
Li 1s
O 1s
C 1s
Si 2p
20.0
60.0
100.0
140.0
180.0
Etching Time (20.00 min/div)

(a)

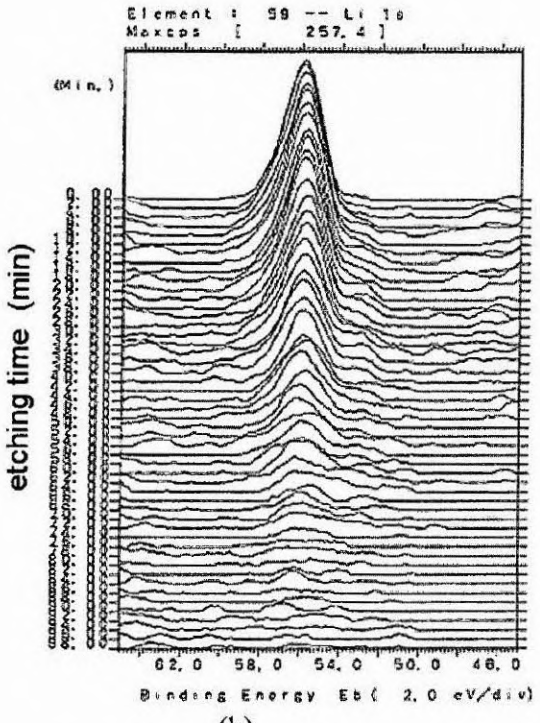
Element : 59 -- Li 1s
Maxcps [257.4]
(Min.)
etching time (min)
62.0
58.0
54.0
50.0
46.0
Binding Energy Eb (2.0 eV/div)

(b)

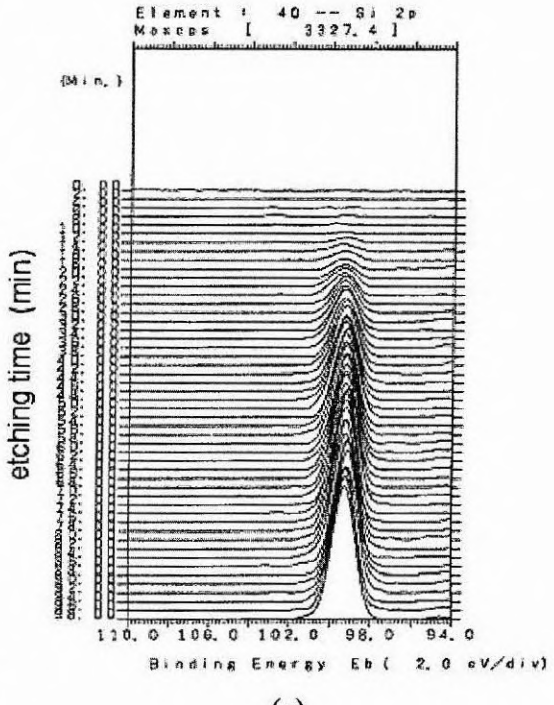
Element : 40 -- Si 2p
Maxcps [3327.4]
(Min.)
etching time (min)
110.0
106.0
102.0
98.0
94.0
Binding Energy Eb (2.0 eV/div)

(c)

Figure 4. (previous page) XPS measurement for Si sample implanted with lithium atoms. (a) atomic concentration; (b) binding energy for Li 1s; (c) binding energy for Si 2p

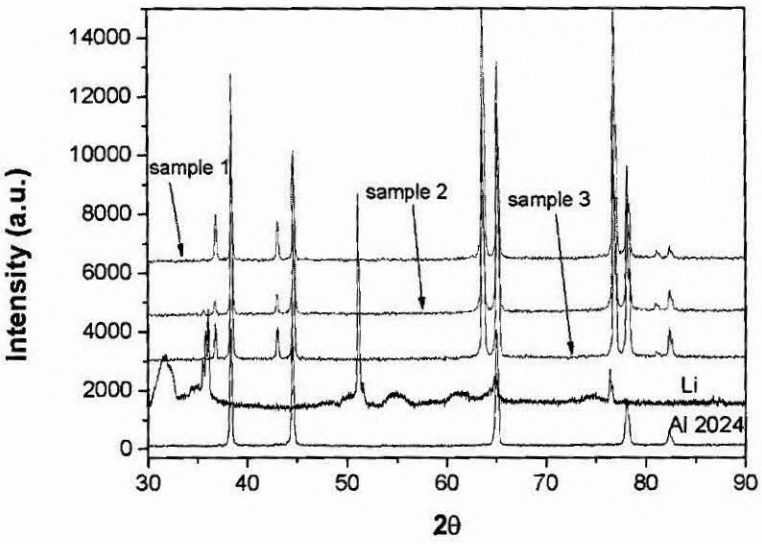

Figure 5. X-ray diffraction for: pure lithium, untreated Al20024 and three samples of Al2024 submitted to PIII&D with lithium atoms in VAST.

References

[1] J. Conrad, J. Appl. Phys. 62 (1987) 777.

[2] M. Nastasi, W. Moller, W. Ensinger, Ion implantation and thin film deposition, in: A. Anders (Ed.), Handbook of Plasma Immersion Ion Implantation and Deposition, John Wiley and Sons, Inc., New York,
2000, p. 125.

[3] J.N. Matossian, R. Wei, J.D. Williams, Surf. Coat. Technol. 96 (1997) 58.

[4] M. Klingenberg, J. Arps, R. Wei, J. Demaree, J. Hirvonen, Surf. Coat. Technol. 158–159 (2002) 164.

[5] A. Öztarhan, I. Brown, C. Bakkaloglu, G. Watt, P. Evans, E. Oks, A. Nikolaev and Z. Tek, Surf.& Coat. Tech., vol. 196 (1-3), pp. 327-332, Jun 2005.

[6] R. M. Oliveira, M. Ueda, J. O. Rossi, B. Diaz and K. Baba, "Plasma Immersion Ion Implantation With Lithium Atoms", IEEE Trans. on Plasma Science – accepted for publication.

[7] R. M. Oliveira, M. Ueda, B. Moreno, L. Hoshida, S. Oswald and E. Abramof, Phys. Stat. Sol. (c) 5, n.4, 893-896 (2008).

[8] R. P. Doerner, M. J. Baldwin, S. I. Krasheninnnikov and D.G. Whyte, *Journal of Nuclear Materials*, 313-316, 383 (2003).
[9] J. M. Howe, Interfaces in Materials: Atomic Structure, Thermodynamics and Kinetics of Solid-Vapor, Solid-Liquid and Solid-Solid Interfaces,Wiley, New York, 17 (1968).
[10] J. O. Rossi, M. Ueda, J. J. Barroso, Braz. Journal of Phys., 34 4B, 1565 (2004).
[11] J. O. Rossi, J. J. Barroso, M. Ueda, G. Silva, IEEE Trans. On Plasma Science, 34, 1757 (2006).
[12] D.L. Chapek, J.R. Conrad, R.J. Matyl, S. B. Felch, "Structural characterization of plasma-doped silicon by high resolution x-ray diffraction", J. Vac. Sci. Technol. B, vol. 12, pp. 951-955 , Mar. 1994.
[13] E. Abramof, A.F. Beloto, M. Ueda, G. F. Gomes, L. A. Berni, H. Reuther, "Analysis of X-ray rocking curves in (001) silicon crystals implanted with nitrogen by plasma immersion ion implantation", Nucl. Instr. & Meth. in Phys. Res. B, vol. 161-163, pp. 1054-1057, Mar. 2000.
[14] B. Diaz, E. Abramof, R. M. Castro, M. Ueda, H. Reuther, "Strain Profile of (001) Silicon Implanted with Nitrogen by Plasma Immersion", Journal of Applied Physics, vol. 101 (10), pp. 103523-103523-6, May 2007.
[15] J. A. Bearden and A. F. Burr, "Reevaluation of X-Ray Atomic Energy Levels," *Rev. Mod. Phys.*, 1967, 39, 125.
[16] C. Fuggle and N. Mårtensson, "Core-Level Binding Energies in Metals," *J. Electron Spectrosc. Relat. Phenom.*, 1980, 21, 275.
[17] D.R. Lide, (Ed.) in *Chemical Rubber Company handbook of chemistry and physics*, CRC Press, Boca Raton, Florida, USA, 81st edition, 2000.